Original Article

Analysis of IGFBP7 expression characteristics in pan-cancer and its clinical relevance to stomach adenocarcinoma

Hui-Wen Xu[#]^, Mei-Qian Wang[#], Sen-Lin Zhu^

Department of Gastroenterology and Hepatology, First Affiliated Hospital of Sun Yat-sen University, Guangzhou, China

Contributions: (I) Conception and design: HW Xu; (II) Administrative support: SL Zhu; (III) Provision of study materials or patients: HW Xu, MQ Wang; (IV) Collection and assembly of data: HW Xu, MQ Wang; (V) Data analysis and interpretation: HW Xu, MQ Wang; (VI) Manuscript writing: All authors; (VII) Final approval of manuscript: All authors.

[#]These authors contributed equally to this work.

Correspondence to: Sen-Lin Zhu, MD, PhD. Department of Gastroenterology and Hepatology, The First Affiliated Hospital, Sun Yat-sen University, 58 Zhongshan 2nd Road, Guangzhou 510080, China. Email: zhusl@mail.sysu.edu.cn.

Background: Insulin-like growth factor (IGF) binding proteins (IGFBPs) are involved in tumorigenesis and cancer progression. IGFBP7 has been shown to act as either a tumor suppressive gene or an oncogene in many tumors, including stomach adenocarcinoma (STAD). To provide a more systematic and comprehensive understanding of IGFBP7 gene, we performed an integrative pan-cancer analysis and explored further with the case of STAD.

Methods: We compared the expression data of IGFBP7 in various cancer and normal tissues obtained from The Cancer Genome Atlas (TCGA) database and the Genotype-Tissue Expression (GTEx) database. The TISIDB web portal was used to analyze the associations of IGFBP7 with cancer molecular subtypes and immune subtypes. We also analyzed the predictive ability and prognostic values of IGFBP7 in pan-cancer, as well as explored its targeted binding proteins and their biological functions. Additionally, we examined the relationship between IGFBP7 and the clinical characteristics of STAD, investigated the co-expression genes and biological functions of differentially expressed genes (DEGs), and validated the mRNA and protein expression levels of IGFBP7 using gastric cancer (GC) and adjacent normal tissues in a small self-case-control study.

Results: IGFBP7 was found to be overexpressed in STAD and downregulated in many other cancers. The mRNA and protein expression levels of IGFBP7 were also significantly higher in the collected GC tissues compared with adjacent tissues. Expression of IGFBP7 varied significantly across molecular subtypes of nine different cancer types and immune subtypes of eight types, with the highest expression observed in the genomically stable molecular subtype and C3 inflammatory immune subtype in STAD. IGFBP7 demonstrated an area under the curve (AUC) >0.7 for predicting 16 cancer types, and an AUC >0.9 for seven types. Patients in the higher IGFBP7 expression group showed a poorer prognosis for adrenal cortical carcinoma (ACC) and low-grade glioma (LGG), while demonstrating a more favorable prognosis for kidney renal clear cell carcinoma (KIRC). IGFBP7 expression in STAD was significantly associated with T stage, pathological stage, histologic grade, and *Helicobacter pylori* infection.

Conclusions: IGFBP7 showed promise as a biomarker for prediction and prognosis in pan-cancer. IGFBP7 was found to be overexpressed in STAD, and its expression was closely associated with the clinical characteristics of STAD.

Keywords: IGFBP7; pan-cancer analysis; stomach adenocarcinoma (STAD)

^ ORCID: Hui-Wen Xu, 0000-0003-4978-5163; Sen-Lin Zhu, 0000-0003-2144-6856.

Submitted Jun 22, 2023. Accepted for publication Sep 21, 2023. Published online Oct 24, 2023.
doi: 10.21037/tcr-23-1055
View this article at: https://dx.doi.org/10.21037/tcr-23-1055

Introduction

Insulin-like growth factor (IGF) binding proteins (IGFBPs) are secreted proteins that include conventional concept of IGFBPs (IGFBP1-6) with high-affinity for IGF, and IGFBP-related proteins (IGFBP-rP1-10) with low-affinity, whose N-terminal domain are similar with that of conventional IGFBPs (1). IGFBPs regulate the biological activity of IGF through binding or dissociating from IGF. They also have IGF-independent effects, influencing cell growth, migration, and metabolism (2,3). Previous reviews have documented the influence of the IGF-IGFR-IGFBP axis and the associations between IGFBPs and gastric cancer (GC) (1,4). Currently, IGFBPs have been implicated in different tumorigenesis and cancer progression (1,5-8).

IGFBP7 is notable of the first IGFBP-related protein (IGFBP-rP1), exhibiting low-affinity with IGF and high-affinity with insulin (9). The expression level and biological role of IGFBP7 vary in different tumor types. IGFBP7 may play a tumor-suppressive role in glioblastoma, hepatocellular carcinoma, and colon cancer (10-13), but can function as an oncogene in head and neck squamous cell carcinomas (HNSC), esophageal adenocarcinoma, lung adenocarcinoma, and bladder cancer (14-17).

GC, primarily composed of stomach adenocarcinoma (STAD), ranks fifth in terms of incidence rate and fourth in terms of mortality rate among common malignancies, making it a burden in tumor diseases (18,19). It was reported that decreased mRNA and protein expression levels of IGFBP7 were associated with poor prognosis in GC (20). However, an opposite finding noticed that advanced GC was characterized by higher mRNA and protein expression of IGFBP7. This increased expression was associated with tumor progression and was considered an independent poor prognostic factor (21). Another study also reported a correlation between increased IGFBP7 mRNA and protein expressions and poor prognosis in GC (22). The discrepancies in the dual roles of IGFBP7 in cancers may arise from the heterogeneity and complexity of tumors.

The main aim of this study is to conduct a systematic and comprehensive analysis of the expression characteristics of IGFBP7 gene in different types of cancer, with a particular emphasis on STAD. This study analyzed IGFBP7 mRNA expression data from The Cancer Genome Atlas (TCGA) and the Genotype-Tissue Expression (GTEx) database, and investigated the associations between IGFBP7 expression and the molecular subtypes and immune subtypes of different cancers. Subsequently, we selected 50 proteins that specifically bind to IGFBP7 and investigated their biological functions. Additionally, we focused on investigating the predictive ability and prognostic values of IGFBP7 in pan-cancer. Furthermore, we explored the relationships between IGFBP7 and the clinical characteristics of STAD. We further examined both the differentially expressed genes (DEGs) and co-expression genes of IGFBP7 in STAD. Additionally, we collected GC tissues and adjacent normal tissues to validate the mRNA and protein expression levels of IGFBP7, as a small self-case-control study. In conclusion, we determine that IGFBP7 has the potential to serve as a predictive and prognostic biomarker in pan-cancer and its expression was closely associated with the clinical characteristics of STAD. We present this article in accordance with the STREGA reporting checklist (available at https://tcr.amegroups.com/article/view/10.21037/tcr-23-1055/rc).

Highlight box

Key findings

- IGFBP7 demonstrated a moderate accuracy of area under the curve (AUC) >0.7 in predicting 16 cancer types and a high accuracy of AUC >0.9 in seven types.
- The expression of IGFBP7 in stomach adenocarcinoma (STAD) was found to have significant relationships with T stage, pathologic stage, histologic grade, and *Helicobacter pylori* infection.

What is known and what is new?

- IGFBP7 expression levels and biological roles vary in different tumor types, including glioblastoma and colon cancer, lung adenocarcinoma and bladder cancer.
- This study conducted a more systematic and comprehensive analysis of IGFBP7 from a pan-cancer perspective.

What is the implication, and what should change now?

- IGFBP7 showed promise as a biomarker for prediction and prognosis in pan-cancer. IGFBP7 was found to be overexpressed in STAD, and its expression was closely associated with the clinical characteristics of STAD.

Methods

Gene expression analysis

The RNA-seq data and relevant clinical data from 15,776 samples across 33 tumor types and normal tissues were downloaded from TCGA database and the GTEx database using UCSC XENA (https://xenabrowser.net/datapages/). The abbreviations for various cancer types are listed in Table S1. The unpaired samples included 414 cases of STAD and 210 cases of normal tissues, while the paired samples consisted of 33 pairs of STADs and para-cancerous tissues. The RNA-seq data from TCGA and GTEx, in transcripts per million (TPM) reads format, were integrated using UCSC XENA, and processed by Toil process (23).

IGFBP7 expression in molecular subtypes and immune subtypes of various cancers

The TISIDB, an integrated repository portal for tumor-immune system interactions, was employed to analyze the correlations between IGFBP7 expression and molecular subtypes or immune subtypes in pan-cancer. The molecular subtypes in pan-cancer were categorized as C1 (wound healing), C2 (IFN-gamma dominant), C3 (inflammatory), C4 (lymphocyte depleted), C5 (immunologically quiet), and C6 (TGF-b dominant) (24).

Protein-protein interaction (PPI) network building

Through in silico analysis of publicly available databases, the proteins with specific binding affinities were identified as targeted binding proteins of IGFBP7. A total of 50 targeted IGFBP7-binding proteins were obtained from the STRING web3 (https://string-db.org/) by using the following main parameters: a minimum required interaction score of "medium confidence (0.400)". Cytoscape version 3.8.2 was used for the visualization of the PPI network.

Gene Ontology (GO) analysis and Kyoto Encyclopedia of Genes and Genomes (KEGG) enrichment analysis

The cluster Profiler package version 3.14.3 was utilized for performing GO and KEGG enrichment analyses on the 50 targeted IGFBP7-binding proteins. Additionally, the org.Hs.eg.db package version 3.10.0 was employed for ID conversion (25,26).

Predictive ability analysis

The predictive ability of IGFBP7 in pan-cancer was assessed using the receiver operating characteristic (ROC) curve. The analysis was performed using the pROC package version 1.17.0.1. An area under the curve (AUC) of 0.5–0.7 indicates low accuracy, an AUC of 0.7–0.9 indicates moderate accuracy, while an AUC above 0.9 indicates high accuracy.

Prognostic value analysis

Kaplan-Meier plots were employed to examine the relationships between IGFBP7 expression and the prognosis of cancers, considering overall survival (OS), disease-specific survival (DSS), and progression-free interval (PFI). Box plots and tables were used to present the expression levels of IGFBP7 in patients with different clinical characteristics in STAD. To identify the prognostic values of IGFBP7 and clinical characteristics in OS, DSS, and PFI, univariate and multivariate Cox regression analyses were conducted. Furthermore, the associations between IGFBP7 expression and prognosis (OS, DSS, and PFI) in different clinical subgroups of STAD were investigated.

The RNA-seq data and related clinical data were downloaded from TCGA database in level 3 HTSeq-fragments per kilobase per million (FPKM) format. Subsequently, the data were converted to TPM format and analyzed after log2 conversion. Visualization was performed using the survminer package version 0.4.9, while statistical analysis was conducted using the survival package version 3.2-10. Cox regression was used for the hypothesis test, with $P<0.05$ indicating statistical significance.

DEGs and co-expression gene analysis of IGFBP7 in STAD

DEGs between different IGFBP7 groups (low expression group: 0–50%; high expression group: over 50%) in STAD were analyzed using the DESeq2 package (27). The volcano map was set with the threshold values of $|\log2 \text{ fold-change (FC)}| > 2.0$ and adjusted P value <0.05. The top 50 co-expression genes, which were positively and negatively correlated with IGFBP7 expression in STAD, were represented in a heat map. Furthermore, GO and KEGG enrichment analyses were performed on the DEGs. The

PPI network of DEGs was analyzed using the STRING web resource, and the top 50 and top 10 hub genes were determined using the MCC algorithm in CytoHubba within Cytoscape.

Immunohistochemistry (IHC)

To validate the results obtained from the public database, 19 pairs of paraffin-embedded GC and adjacent normal gastric tissues were obtained from the First Affiliated Hospital of Sun Yat-sen University, which received ethical approval from the Ethics Committee of our hospital (approval number: No. 279, 2021). This study was conducted in accordance with the Declaration of Helsinki (as revised in 2013). Written informed consent was obtained from all patients. Tissue samples were obtained in adherence to ethical and legal standards.

Immunohistochemical staining of IGFBP7 (Cat#:ab74169, Abcam, Cambridge, UK) was performed at a concentration of 1:800. The IHC score was calculated based on the staining intensity and the proportion of stained cells. The staining intensity was scored on a scale from 0 to 3 (0 = negative staining; 1 = weak; 2 = moderate; 3 = strong). The percentage of positive staining cells was scored of 0 to 4 points (0 = none; 1 = 1–25%; 2 = 26–50%; 3 = 51–75%; 4 =76–100%). The IHC score was computed by multiplying the intensity score by the proportion score, resulting in a range of 0 to 12. Tissues with an IHC score greater than 4 were classified as having high IGFBP7 expression (28).

RNA extraction, reverse transcription and quantitative reverse transcriptase polymerase chain reaction (qRT-PCR)

Total RNA was extracted from tissues using Trizol reagent (Invitrogen, USA) following the manufacturer's instructions. The extracted RNA was then treated with RNase-free DNase. For qRT-PCR, 2× SYBR Green qPCR Master Mix (EZBioscience) was used. The qRT-PCR reactions were performed on a CFX96 Touch Real-time PCR Detection System (Bio-Rad, CA, USA) (29). The following forward (F) and reverse (R) primers were used for amplification: IGFBP7, F 5'-CGA GCA AGG TCC TTC CAT AGT-3' and R 5'-GGT GTC GGG ATT CCG ATG AC-3'; and glyceraldehyde-3-phosphate dehydrogenase (GAPDH), F 5'-GTC TCC TCT GAC TTC AAC AGC G-3' and R 5'-ACC ACC CTG TTG CTG TAG CCA A-3'. Relative quantification and statistical analysis were performed using the $2^{-\Delta\Delta Ct}$ method.

Statistical analysis

Statistical analysis was conducted using R software version 3.6.3. The ggplot2 package and GraphPad Prism version 8.0.2 were utilized for data visualization. The unpaired samples were analyzed using the Wilcoxon rank sum test, while the paired samples were analyzed using the Wilcoxon signed rank test. For statistical significance, a P value <0.05 was considered significant. The following notations were used: ns (not significant, P≥0.05), * (P<0.05), ** (P<0.01), and *** (P<0.001).

Results

Differential expressions of IGFBP7 in pan-cancer

We compared the expression of IGFBP7 in TCGA tumors with the data of GTEx database. We found that IGFBP7 was downregulated in 14 cancer types (BLCA, BRCA, COAD, ESCA, CESC, KICH, LUAD, LUSC, PRAD, SARC, TGCT, THCA, UCEC, and UCS), and upregulated in 13 types (CHOL, DLBC, GBM, HNSC, LAML, LGG, LIHC, MESO, PAAD, SKCM, STAD, THYM, and UVM) (*Figure 1A*). Furthermore, when comparing TCGA tumors with adjacent normal tissues, IGFBP7 was downregulated in nine cancer types (BLCA, KICH, KIRC, KIRP, LUAD, LUSC, PRAD, THCA, and UCEC) and upregulated in four types (COAD, ESCA, HNSC, and STAD) (*Figure 1B*). In the twice comparisons, IGFBP7 was found to be overexpressed in HNSC and STAD, while it was downregulated in BLCA, KICH, LUAD, LUSC, PRAD, THCA, and UCEC.

Correlations between IGFBP7 and molecular or immune subtypes in pan-cancer

We observed variations in the expression of IGFBP7 across different molecular subtypes in nine cancer types (BRCA, HNSC, LGG, LIHC, LUSC, OV, PCPG, STAD, and UCEC) (*Figure 2A-2I*). Notably, in the case of STAD, the highest expression of IGFBP7 was observed in the genomically stable molecular subtype (*Figure 2H*). Additionally, we identified distinct IGFBP7 expressions across immune subtypes in eight cancer types (BRCA, LGG, LIHC, LUSC, PCPG, PRAD, STAD, and UCEC) (*Figure 3A-3H*). For STAD, the C3 inflammatory subtype

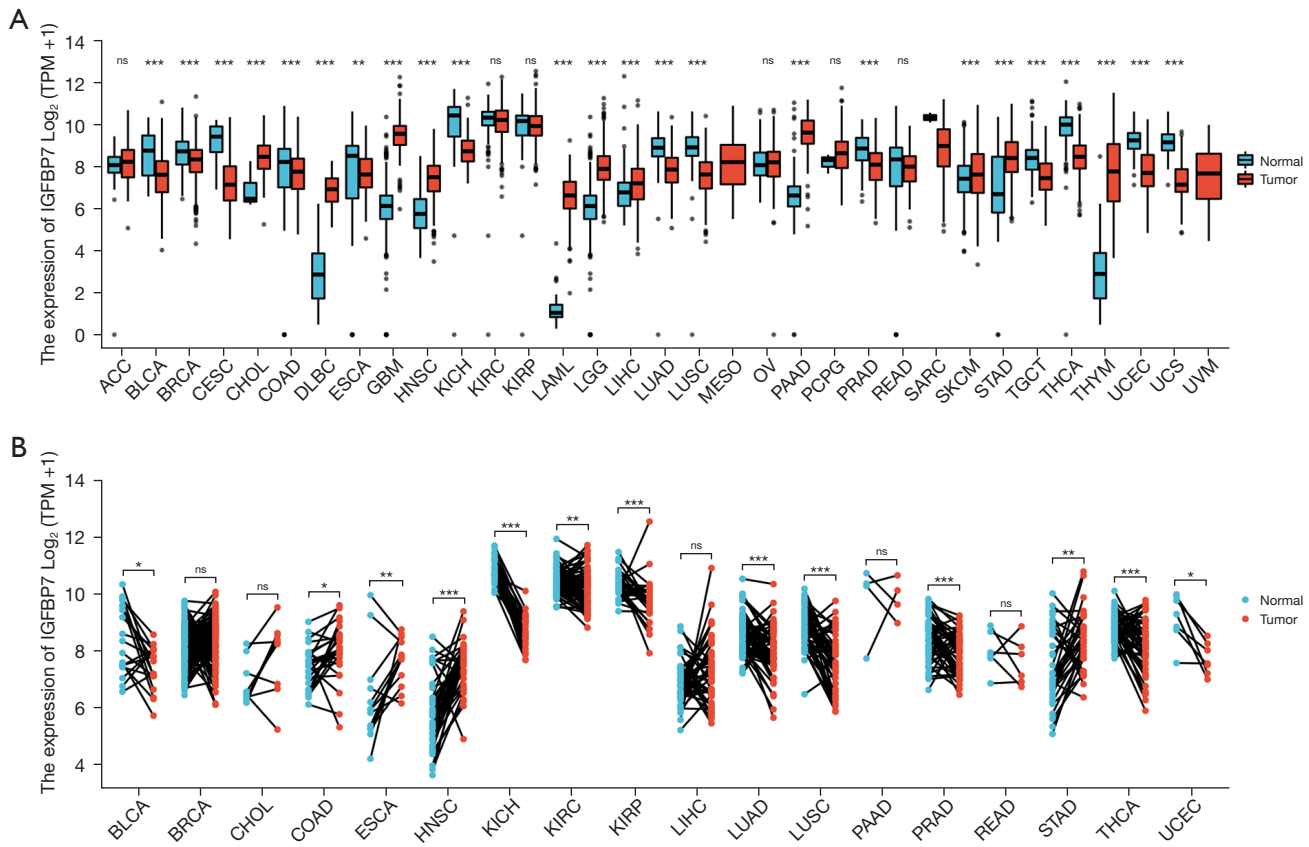

Figure 1 The expression levels of IGFBP7 in tumors and normal tissues obtained from TCGA (A) and the GTEx database (B). ns, not significant, P≥0.05; *, P<0.05; **, P<0.01; ***, P<0.001. TPM, transcripts per million; TCGA, The Cancer Genome Atlas; GTEx, Genotype-Tissue Expression.

exhibited the highest expression of IGFBP7 (*Figure 3G*).

PPI network and GO and KEGG enrichment analyses

We presented a visual representation consisting of 50 targeted binding proteins of IGFBP7 (*Figure 4A*). The top three biological functions of these proteins were determined through GO and KEGG enrichment analyses (*Figure 4B,4C*). The enrichment analysis revealed that the biological process (BP) was primarily associated with insulin-like growth factor receptor (IGFR), regulation of IGFR, and positive regulation of IGFR. The cellular component (CC) was found to encompass the secretory granule lumen, platelet alpha granule lumen, and cytoplasmic vesicle lumen. In terms of molecular function (MF), the proteins were involved in IGF-I binding, IGF binding, and growth factor binding. Additionally, the KEGG pathway enrichment analysis revealed associations with proteoglycans in cancer, focal adhesion, and MAPK signaling pathway.

Predictive ability of IGFBP7 in pan-cancer

IGFBP7 demonstrated a moderate level of accuracy (AUC >0.7) in predicting 16 different cancer types in pan-cancer analysis (*Figure 5A-5P*). Specifically, it exhibited a high accuracy (AUC >0.9) in seven cancer types, namely DLBC, GBM, GBMLGG, LGG, PAAD, THCA, and THYM. Notably, the ability of IGFBP7 to predict STAD resulted in an AUC value of 0.771 (*Figure 5M*).

Prognostic value of IGFBP7 in various cancers

The expression levels of IGFBP7 exhibited notable correlations with the OS, DSS, and PFI in adrenal cortical carcinoma (ACC), kidney renal clear cell carcinoma (KIRC),

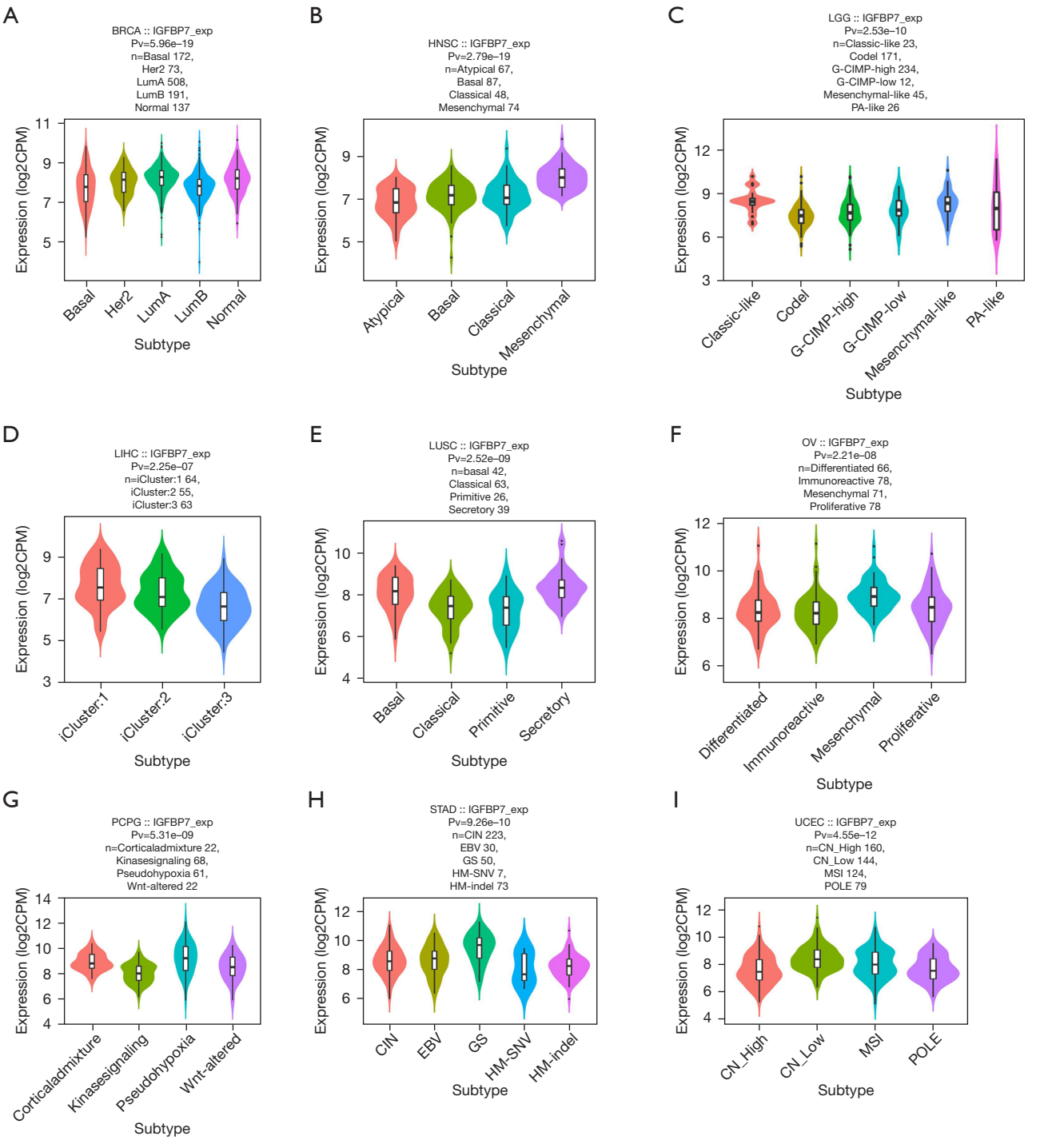

Figure 2 The correlations between the expression of IGFBP7 and molecular subtypes across TCGA tumors. TCGA, The Cancer Genome Atlas; G-CIMP, CpG island methylator phenotype; PA, pilocytic astrocytoma; CIN, chromosomal instability; EBV, Epstein-Barr virus; GS, genomically stable; HM, hypermutation; SNV, single nucleotide variants; CN, copy number; MSI, microsatellite instability; POLE, DNA polymerase epsilon.

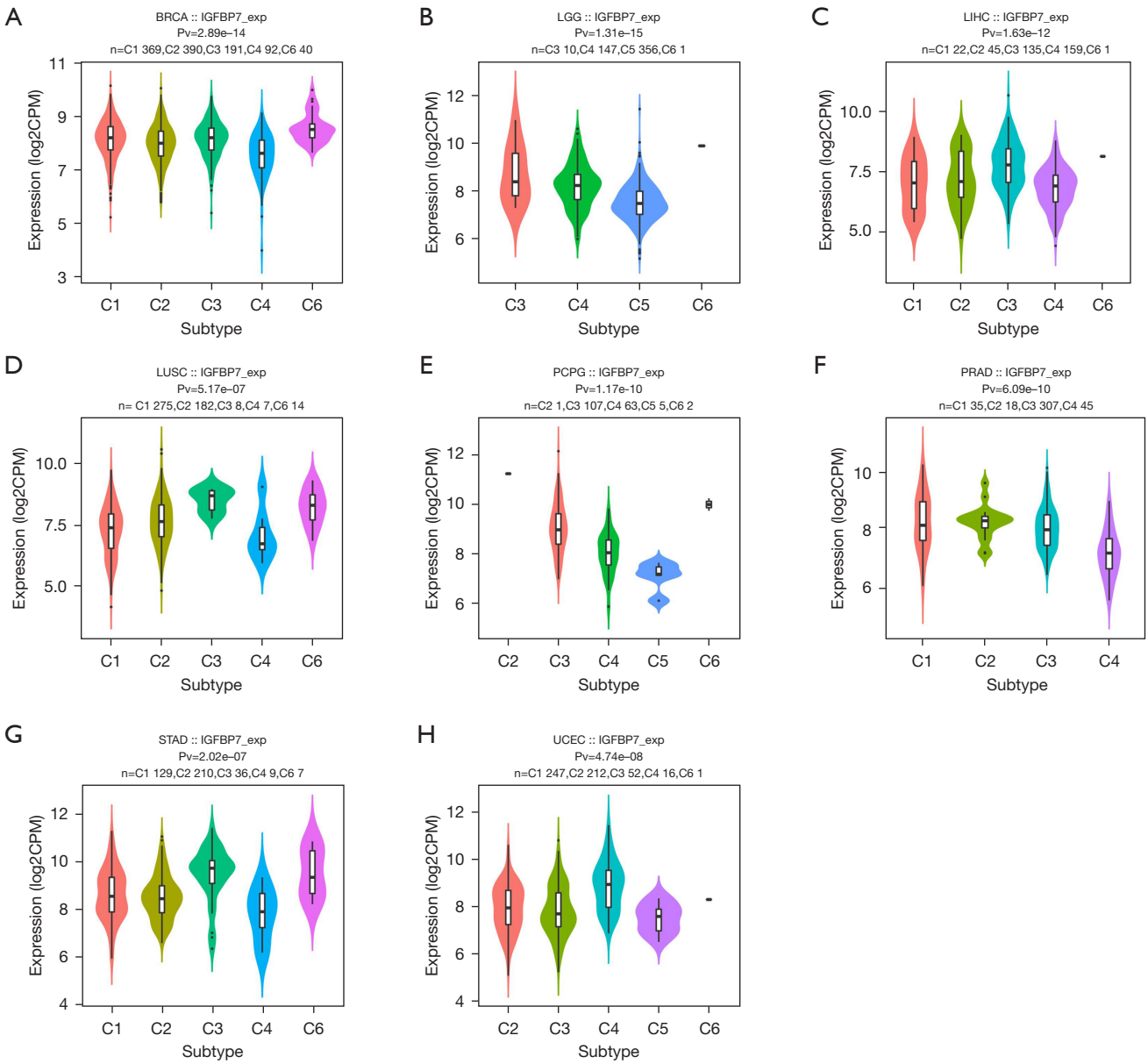

Figure 3 The correlations between the expression of IGFBP7 and immune subtypes across TCGA tumors. TCGA, The Cancer Genome Atlas.

and low-grade glioma (LGG) (*Figure 6A-6I*). Patients with higher expression of IGFBP7 had worse prognosis in ACC and LGG, whereas those with higher IGFBP7 expression in KIRC had a better prognosis. However, no significant differences were observed in the prognosis of STAD patients based on different levels of IGFBP7 expression (*Figure 6J-6L*).

We performed analyses to assess the associations between IGFBP7 expression and various clinical characteristics in STAD. Our findings indicated a significant correlation between IGFBP7 expression and T stage, pathologic stage, histologic grade, and *Helicobacter pylori* (*H. pylori*) infection (*Table 1*). IGFBP7 expression was notably higher in STAD patients with *H. pylori* infection, compared with healthy individuals and patients without infection (*Figure 7A*). Additionally, IGFBP7 showed remarkable overexpression in the G2 and G3 groups (*Figure 7B*), stage II–IV (*Figure 7C*), and T 2–4 (*Figure 7D*). We further investigated the

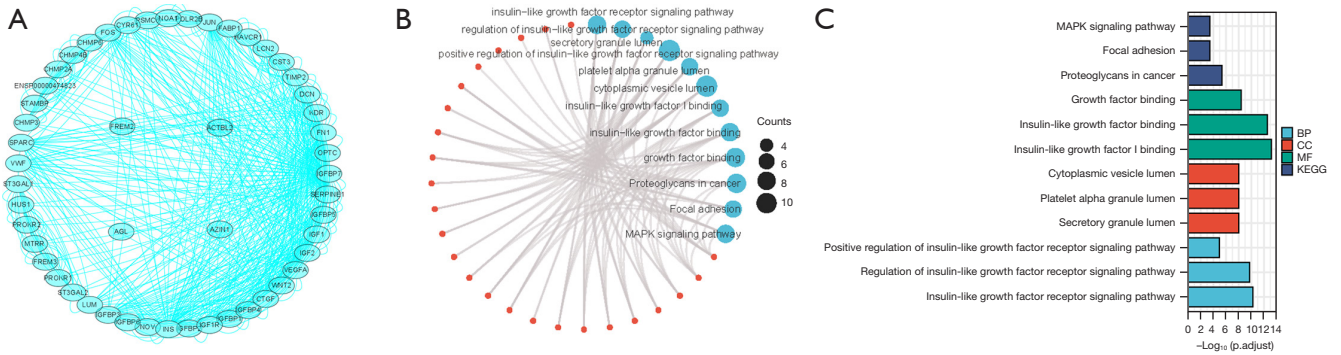

Figure 4 The PPI network (A), as well as the GO (B) and KEGG analyses (C) of the 50 targeted binding proteins of IGFBP7. PPI, protein-protein interaction; GO, Gene Ontology; KEGG, Kyoto Encyclopedia of Genes and Genomes; BP, biological process; CC, cellular component; MF, molecular function.

correlations of IGFBP7 expression with prognosis among these distinct clinical subgroups of STAD. However, no differences were observed in prognosis based on OS, DSS, and PFI (Figure S1).

Furthermore, we conducted univariate and multivariate Cox regression analyses. Tumor, Node, Metastasis (TNM) stage, pathologic stage, and age were found to be significantly associated with OS (*Table 2*). Similarly, TNM stage, pathologic stage, and gender showed associations with DSS (Table S2). With regard to PFI, all factors, except for histologic grade, exhibited correlations (Table S3).

DEGs and co-expression gene analysis of IGFBP7 in STAD

A total of 343 DEGs were identified in this study. These genes met the threshold values of |log2FC| >2.0 and adjusted P<0.05. Among these DEGs, 261 genes were upregulated and 82 genes were downregulated (*Figure 8A*). To further investigate the relationship between IGFBP7 expression and other genes, we performed a co-expression analysis and generated a heat-map (Figure S2). The heat-map displays the top 50 genes that positively or negatively correlated with IGFBP7 expression in STAD. The top 10 positively correlated genes included *THBS4*, *MGP*, *MYLK*, *COL14A1*, *HAND2-AS1*, *INMT*, *CNN1*, *ANGPTL1*, *MYL9*, and *POPDC2*. On the other hand, the top 10 negatively correlated genes included *CLCA4*, *IL36RN*, *CRNN*, *S100A7*, *SPRR2D*, *KRT78*, *KRT13*, *WFDC5*, *DYANP*, and *S100A7A*.

In order to gain insight into the biological functions of these DEGs, we performed GO and KEGG pathway analyses (*Figure 8B*). The BP that were primarily affected by the DEGs included muscle system processes, muscle contraction, and cornification. The CC enriched with these DEGs were collagen-containing extracellular matrix, contractile fiber, and contractile fiber part. The MF of these genes were mainly associated with receptor ligand activity, glycosaminoglycan binding, and extracellular matrix structural constituent. The KEGG pathway analysis revealed that the DEGs were involved in neuroactive ligand-receptor interaction, vascular smooth muscle contraction, and renin secretion.

Furthermore, we identified the top 50 hub genes among the DEGs and examined their distribution in three regions (*Figure 8C*). The top 10 hub genes, which play important roles in the network of the DEGs, were IVL, LCE3D, SPRR2E, SPRR3, SPRR2B, SPRR2A, LCE3E, SPRR2D, SPRR2G, and SPRR2F (*Figure 8D*). These hub genes may have key regulatory functions in STAD, based on their interaction patterns with other DEGs.

Verification of over-expression of IGFBP7 in STAD

To verify the over-expression of IGFBP7 in STAD according to TCGA results, we collected 19 pairs of GC tissues and adjacent normal tissues. IGFBP7 mRNA and protein expression levels were analyzed using qRT-PCR and IHC. The expression of IGFBP7 mRNA was significantly higher in GC tissues compared with adjacent tissues (*Figure 9A*). The staining intensity of IGFBP7 protein was significantly stronger in GC tissues (*Figure 9B*).

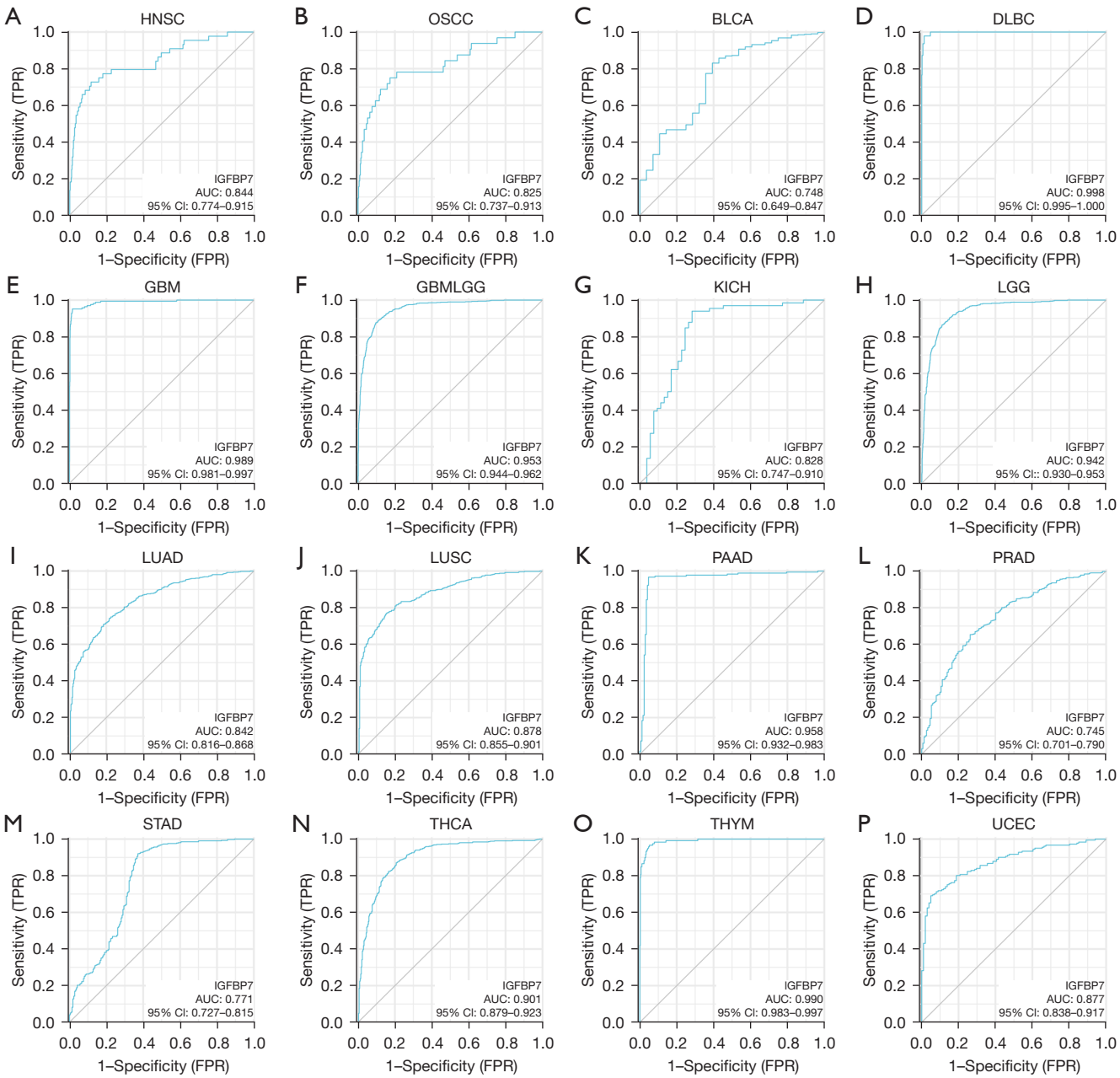

Figure 5 The ROC curve for IGFBP7 expression in various pan-cancer cases. ROC, receiver operating characteristic; FPR, false positive rate; TPR, true positive rate; AUC, area under the curve; CI, confidence interval.

Discussion

From a pan-cancer perspective, we observed overexpression of IGFBP7 in HNSC and STAD, while it was under-expressed in BLCA, KICH, LUAD, LUSC, PRAD, THCA, and UCEC. The mutant *Igfbp7* and *Trp53* genes were found to induce lung squamous cell carcinoma (LUSC) in a murine model (30). The expression of *Igfbp7* gene was reduced or even absent in follicular thyroid cancer and anaplastic thyroid cancer. It was shown to inhibit cell proliferation in thyroid carcinoma (THCA) through downregulation of AKT activity and suppression of cell cycle progression (31). In HNSC, 10 hub genes were identified from the co-expressed genes of BGN,

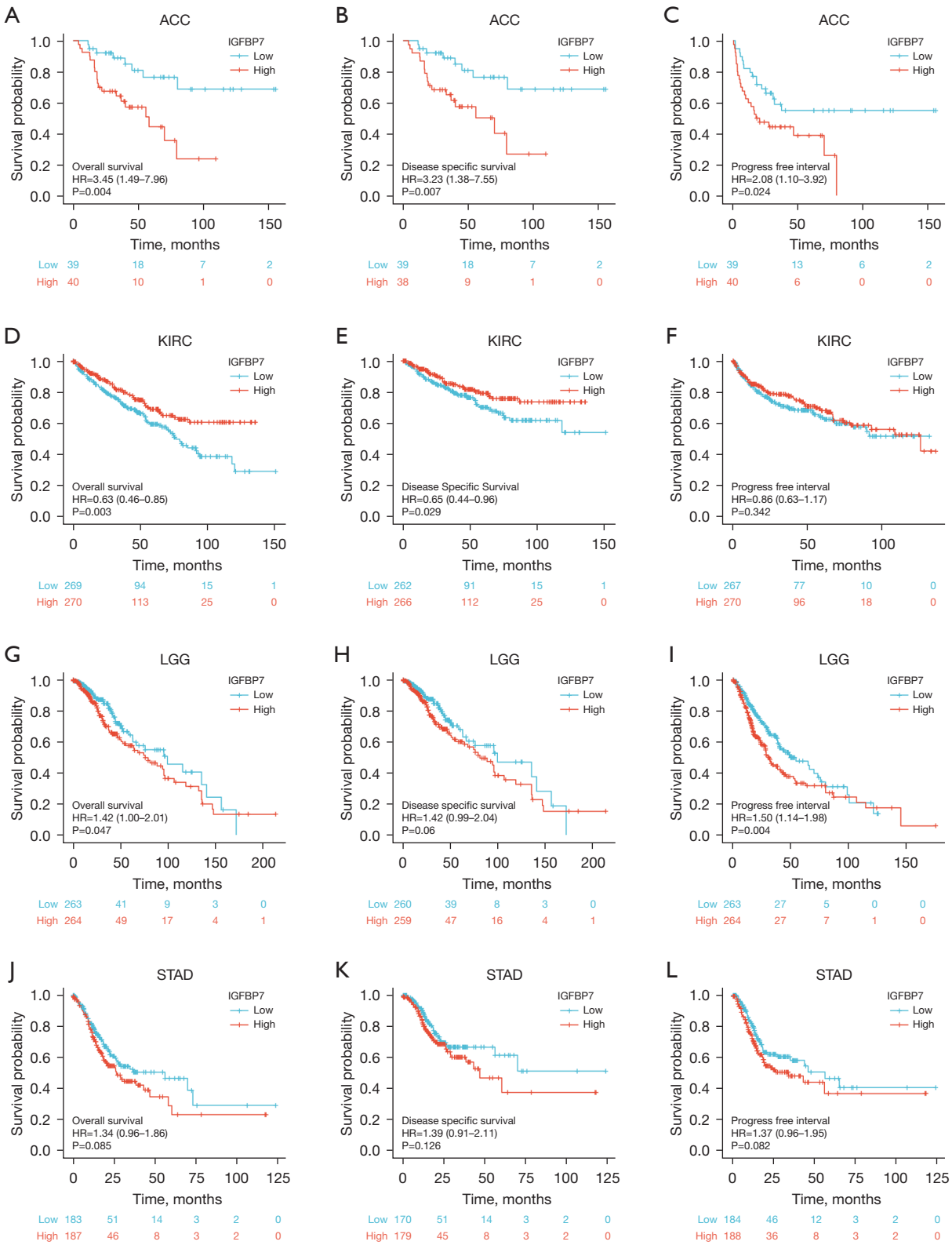

Figure 6 The correlations between the expression of IGFBP7 and the prognosis (OS, DSS, and PFI) of four cancer types: ACC (A-C), KIRC (D-F), LGG (G-I), and STAD (J-L). OS, overall survival; DSS, disease-specific survival; PFI, progression-free interval; HR, hazard ratio.

Table 1 The clinical characteristics of patients with STAD categorized according to the expression level of IGFBP7

Characteristics	Low expression of IGFBP7 (n=187)	High expression of IGFBP7 (n=188)	P
T stage, n (%)			0.012*
T1	16 (4.4)	3 (0.8)	
T2	43 (11.7)	37 (10.1)	
T3	76 (20.7)	92 (25.1)	
T4	49 (13.4)	51 (13.9)	
Gender, n (%)			0.884
Female	68 (18.1)	66 (17.6)	
Male	119 (31.7)	122 (32.5)	
Age (years), n (%)			0.437
≤65	78 (21.0)	86 (23.2)	
>65	108 (29.1)	99 (26.7)	
Pathologic stage, n (%)			0.029*
Stage I	36 (10.2)	17 (4.8)	
Stage II	48 (13.6)	63 (17.9)	
Stage III	73 (20.7)	77 (21.9)	
Stage IV	20 (5.7)	18 (5.1)	
Histologic grade, n (%)			0.005*
G1	6 (1.6)	4 (1.1)	
G2	83 (22.7)	54 (14.8)	
G3	95 (26.0)	124 (33.9)	
Reflux history, n (%)			0.950
No	95 (44.4)	80 (37.4)	
Yes	22 (10.3)	17 (7.9)	
H. pylori infection, n (%)			0.038*
No	97 (59.5)	48 (29.4)	
Yes	7 (4.3)	11 (6.7)	

The table provides percentage summaries of totals, automatically handling invalid data. *, P<0.05. STAD, stomach adenocarcinoma.

which is rich in leucine small protein polysaccharides. *Igfbp*7 was one of the hub genes, and its expression was significantly increased (32). The *Igfbp*7 gene became activated during gastric tumorigenesis, and its protein expression level increased as the disease progressed (33). IGFBP7 promoted GC by enhancing polarization of tumor-associated macrophages and M2 macrophages, which was mediated through the FGF2/FGFR1/PI3K/AKT axis (34). The epigenetic downregulation of IGFBP7 led to its overexpression in GC cells, which in turn induced growth inhibition and apoptosis (35) . The contradictory expressions and roles of IGFBP7 in STAD deserve attention in the future.

Furthermore, IGFBP7 expression varied significantly among molecular subtypes of nine cancer types and immune subtypes of eight types. IGFBP7 demonstrated a moderate accuracy of AUC >0.7 in predicting 16 cancer types and a high accuracy of AUC >0.9 in seven types. ACC and LGG patients exhibited a worse prognosis in the high IGFBP7 expression group, whereas KIRC patients with higher

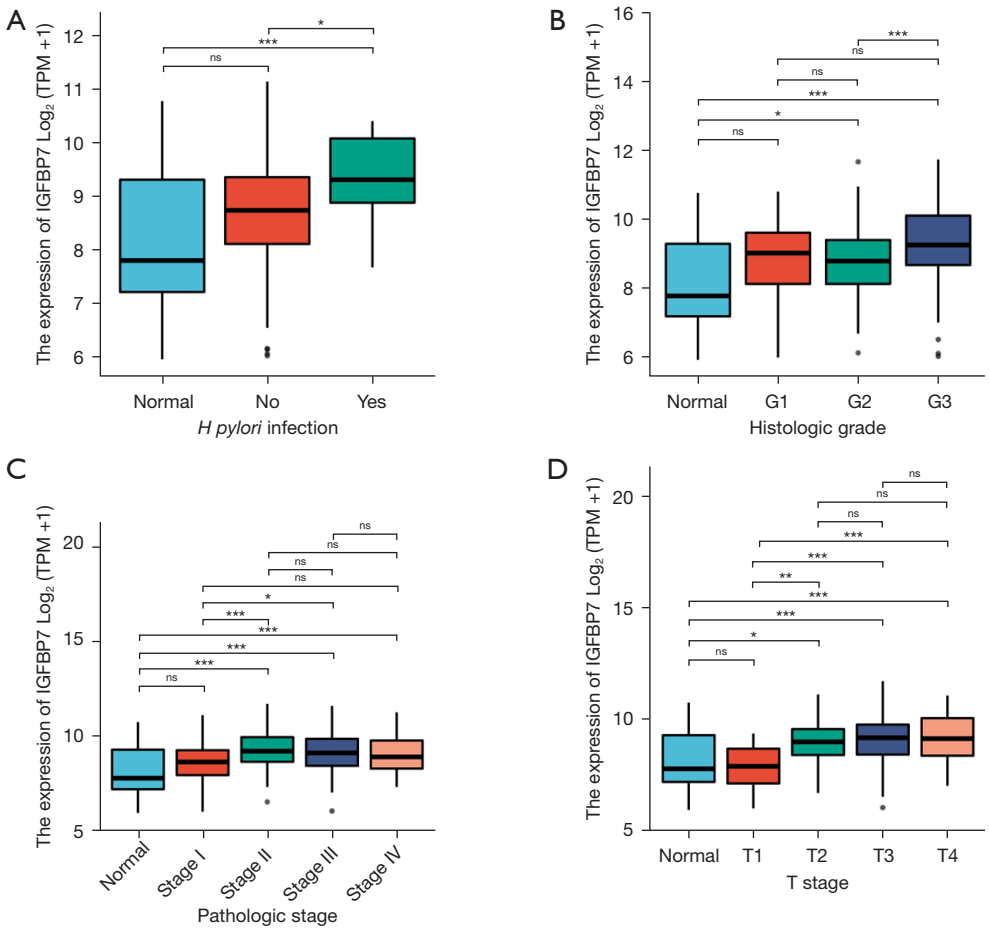

Figure 7 The different expression levels of IGFBP7 among four types of clinical characteristics in patients with STAD. ns, not significant, P≥0.05; *, P<0.05; **, P<0.01; ***, P<0.001. TPM, transcripts per million; STAD, stomach adenocarcinoma.

Table 2 The results of univariate and multivariate Cox regression analyses conducted to investigate the impact of clinical characteristics on the OS of STAD patients

Characteristics	Total (N)	Univariate analysis		Multivariate analysis	
		HR (95% CI)	P value	HR (95% CI)	P value
T stage (T3 and T4 *vs.* T2 and T1)	362	1.719 (1.131–2.612)	0.011	1.174 (0.672–2.052)	0.573
N stage (N1, N2, N3 *vs.* N0)	352	1.925 (1.264–2.931)	0.002	1.532 (0.913–2.569)	0.106
M stage (M1 *vs.* M0)	352	2.254 (1.295–3.924)	0.004	2.185 (1.194–3.998)	0.011
Pathologic stage (II, III, IV *vs.* I)	347	2.247 (1.210–4.175)	0.010	1.535 (0.591–3.988)	0.379
Age (>65 *vs.* ≤65 years)	367	1.620 (1.154–2.276)	0.005	1.806 (1.247–2.615)	0.002
Gender (male *vs.* female)	349	1.267 (0.891–1.804)	0.188		
Histologic grade (G2, G3 *vs.* G1)	361	1.957 (0.484–7.910)	0.346		
Reflux history (yes *vs.* no)	213	0.582 (0.291–1.162)	0.125		
H. pylori infection (yes *vs.* no)	162	0.650 (0.279–1.513)	0.317		

OS, overall survival; STAD, stomach adenocarcinoma; HR, hazard ratio; CI, confidence interval.

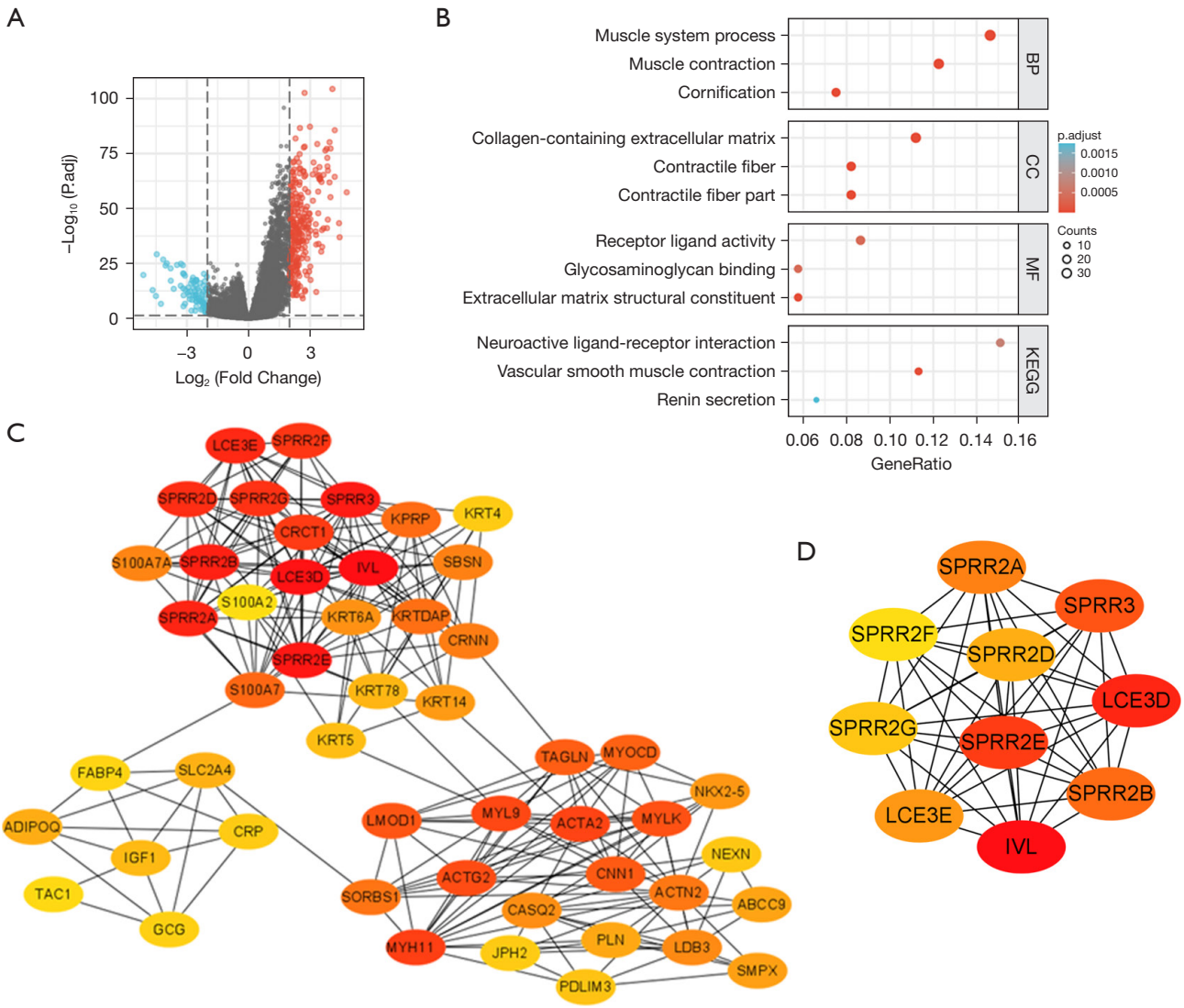

Figure 8 The analyses of DEGs based on the high and low expression groups of IGFBP7 in STAD. (A) shows the Volcano map, where red points represent upregulation and blue points represent downregulation. (B) displays the GO and KEGG enrichment analyses. (C) presents the top 50 hub genes, while (D) illustrates the top 10 hub genes. DEGs, differentially expressed genes; STAD, stomach adenocarcinoma; GO, Gene Ontology; KEGG, Kyoto Encyclopedia of Genes and Genomes; BP, biological process; CC, cellular component; MF, molecular function.

IGFBP7 expression had a better prognosis.

Moreover, the biological functions of 50 targeted IGFBP7-binding proteins were associated with the IGFR-related signaling pathway, proteoglycans in cancer, focal adhesion, and the MAPK signaling pathway. Notably, insulin, insulin receptor, IGF, and IGFR play a major role in STAD (36-39). IGFBP7 were enriched in the signaling pathways of focal adhesion, extracellular matrix structural constituents, cell-substratum junctions, extracellular structures, and matrix organization (40). The effects of IGFBP7 and its targeted binding proteins on various cancers warrant further research in the future.

In this study, we placed particular emphasis on IGFBP7 in the context of STAD. IGFBP7 showed overexpression in STAD, particularly in the genomically stable molecular subtype and the C3 inflammatory immune subtype. Additionally, the mRNA and protein expression levels of IGFBP7 were significantly higher in the obtained GC tissues

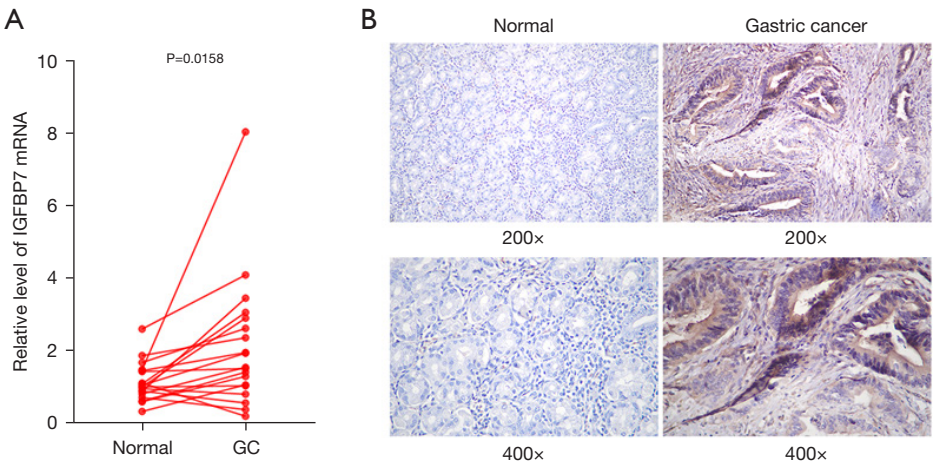

Figure 9 The expression levels of IGFBP7 mRNA and protein in collected GC and adjacent normal tissues by hematoxylin-eosin staining. (A) shows the qRT-PCR analysis of IGFBP7 mRNA expression, while (B) presents representative micrographs of IGFBP7 protein expression. GC, gastric cancer; qRT-PCR, quantitative reverse transcriptase polymerase chain reaction.

compared with the adjacent tissues. The experimental results mentioned above confirmed a significant increase in IGFBP7 expression in GC tissue, which was consistent with the finding from the testing with the TCGA datasets.

IGFBP7 demonstrated an AUC of 0.771 in predicting STAD. The serum levels of IGFBP7 showed a predictive value of 0.774 in identifying GC patients (41). Despite the lack of significant differences in OS, DSS, and PFI among patients with STAD, the expression of IGFBP7 was significantly associated with T stage, pathologic stage, histologic grade, and *H. pylori* infection. *H. pylori* is recognized as the main risk factor for STAD, leading to chronic inflammation and activation of cancer-related signaling pathways (42). The elevated expression and predictive ability of IGFBP7, along with the significant association with clinical characteristics, were generally consistent with the findings of a comprehensive analysis on IGFBPs (IGFBP1-7) in patients with GC (40). Additionally, univariate and multivariate Cox regression analyses revealed that clinical stage T 2–4, pathologic stage II–IV, and age >65 were identified as risk factors for OS, DSS, and PFI in patients with STAD. Therefore, we concluded that IGFBP7 was closely associated with STAD clinically.

After applying the designated threshold values, we identified 261 upregulated DEGs and 82 downregulated DEGs in STAD. Through the screening process of the top 50 positively or negatively co-expressed DEGs of IGFBP7, we observed that all 50 positive genes showed significant correlation, while 29 negative genes exhibited a significant correlation. Furthermore, our analysis of the biological functions of 343 DEGs indicated that BP were primarily associated with muscle system processes, muscle contraction, and cornification. MF were primarily focused on receptor-ligand activity, glycosaminoglycan binding, and extracellular matrix structural constituents. KEGG analyses revealed enrichment in neuroactive ligand-receptor interactions, vascular smooth muscle contraction, and renin secretion.

Additionally, the top 50 hub genes of the DEGs were distributed across three regions, which may suggest diverse collaborative effects. Among the top 10 hub genes including IVL, all were downregulated in STAD, and among them, only SPRR3, SPRR2D, and SPRR2G exhibited a significant correlation with IGFBP7. Involucrin (IVL), a component of the keratinocyte cross-linked envelope, is located in the cytoplasm and undergoes cross-linking with membrane proteins by transglutaminase (43). In a documented case of stomach adenosquamous carcinoma, immunohistochemical findings revealed that adenocarcinoma cells tested positive for the secretory component and carcinoembryonic antigen (CEA), but negative for IVL. In contrast, the squamous cell carcinoma component displayed positive staining for IVL and negative staining for CEA (44). SPRR3, SPRR2D, and SPRR2G are small proline-rich proteins (SPRR) that exhibit overexpression in squamous tissue, potentially implicating their involvement in the process of keratinization and wound healing (45). Currently, there are no research reports on the association of SPRR with GC or

STAD. Exploring the co-expression genes and biological functions of DEGs based on the expression level of IGFBP7 could provide valuable insights for STAD.

Our study has encountered several limitations. Our exploration of IGFBP7 in various cancers relied solely on computational methods using the TCGA and GTEx databases. Future verification of the biological functions of IGFBP7 in STAD requires a thorough examination and experimentation using both clinical data and biological analyses.

Conclusions

In this study, we investigated the expression levels and clinical significance of IGFBP7 across various types of cancer, with a particular focus on STAD. Using data from TCGA, IGFBP7 was overexpressed in patients with STAD, a finding that was confirmed through qRT-PCR and IHC experiments. Additionally, IGFBP7 expression was highest in the genomically stable molecular subtype and the C3 inflammatory immune subtype of STAD. Moreover, IGFBP7 demonstrated moderate accuracy of AUC >0.7 in predicting 16 different cancer types, with particularly high accuracy of AUC >0.9 in seven types. Furthermore, IGFBP7 showed significant associations with various clinical parameters such as T stage, pathologic stage, histologic grade, and *H. pylori* infection. In addition, we investigated the binding proteins targeted by IGFBP7 and the biological functions of DEGs in STAD. In conclusion, our study demonstrated that IGFBP7 held promise as a biomarker for the prediction and prognosis of various cancers. Specifically, in the case of STAD, IGFBP7 was overexpressed and appeared to be clinically relevant.

Acknowledgments

Funding: This study was supported by Guangzhou Science and Technology Development Funds (Key Program, No. 201803010103).

Footnote

Reporting Checklist: The authors have completed the STREGA reporting checklist. Available at https://tcr.amegroups.com/article/view/10.21037/tcr-23-1055/rc

Data Sharing Statement: Available at https://tcr.amegroups.com/article/view/10.21037/tcr-23-1055/dss

Peer Review File: Available at https://tcr.amegroups.com/article/view/10.21037/tcr-23-1055/prf

Conflicts of Interest: All authors have completed the ICMJE uniform disclosure form (available at https://tcr.amegroups.com/article/view/10.21037/tcr-23-1055/coif). All authors report receiving funding from Guangzhou Science and Technology Development Funds (Key Program, No. 201803010103). The authors have no other conflicts of interest to declare.

Ethical Statement: The authors are accountable for all aspects of the work and in ensuring that questions related to the accuracy or integrity of any part of the work are appropriately investigated and resolved. The study was conducted in accordance with the Declaration of Helsinki (as revised in 2013). The study was approved by the Ethics Committee of the First Affiliated Hospital of Sun Yat-sen University (approval number: No. 279, 2021) and informed consent was obtained from all individual participants.

References

1. Kashyap MK. Role of insulin-like growth factor-binding proteins in the pathophysiology and tumorigenesis of gastroesophageal cancers. Tumour Biol 2015;36:8247-57.
2. Holly J, Perks C. The role of insulin-like growth factor binding proteins. Neuroendocrinology 2006;83:154-60.
3. Song F, Zhou XX, Hu Y, et al. The Roles of Insulin-Like Growth Factor Binding Protein Family in Development and Diseases. Adv Ther 2021;38:885-903.
4. Liu H, Gu H, Kutbi EH, et al. Association of IGF-1 and IGFBP-3 levels with gastric cancer: A systematic review and meta-analysis. Int J Clin Pract 2021;75:e14764.
5. Yi HK, Hwang PH, Yang DH, et al. Expression of the insulin-like growth factors (IGFs) and the IGF-binding proteins (IGFBPs) in human gastric cancer cells. Eur J Cancer 2001;37:2257-63.

6. Minchenko OH, Kharkova AP, Minchenko DO, et al. Effect of hypoxia on the expression of genes that encode some IGFBP and CCN proteins in U87 glioma cells depends on IRE1 signaling. Ukr Biochem J 2015;87:52-63.
7. Bei Y, Huang Q, Shen J, et al. IGFBP6 Regulates Cell Apoptosis and Migration in Glioma. Cell Mol Neurobiol 2017;37:889-98.
8. Thomas D, Radhakrishnan P. Role of Tumor and Stroma-Derived IGF/IGFBPs in Pancreatic Cancer. Cancers (Basel) 2020;12:1228.
9. Burger AM, Leyland-Jones B, Banerjee K, et al. Essential roles of IGFBP-3 and IGFBP-rP1 in breast cancer. Eur J Cancer 2005;41:1515-27.
10. Pen A, Durocher Y, Slinn J, et al. Insulin-like growth factor binding protein 7 exhibits tumor suppressive and vessel stabilization properties in U87MG and T98G glioblastoma cell lines. Cancer Biol Ther 2011;12:634-46.
11. Tian X, Zhang L, Sun L, et al. Low expression of insulin-like growth factor binding protein 7 associated with poor prognosis in human glioma. J Int Med Res 2014;42:651-8.
12. Akiel M, Guo C, Li X, et al. IGFBP7 Deletion Promotes Hepatocellular Carcinoma. Cancer Res 2017;77:4014-25.
13. Li Y, Xi Y, Zhu G, et al. Downregulated IGFBP7 facilitates liver metastasis by modulating epithelial mesenchymal transition in colon cancer. Oncol Rep 2019;42:1935-45.
14. Sepiashvili L, Hui A, Ignatchenko V, et al. Potentially novel candidate biomarkers for head and neck squamous cell carcinoma identified using an integrated cell line-based discovery strategy. Mol Cell Proteomics 2012;11:1404-15.
15. Smith E, Ruszkiewicz AR, Jamieson GG, et al. IGFBP7 is associated with poor prognosis in oesophageal adenocarcinoma and is regulated by promoter DNA methylation. Br J Cancer 2014;110:775-82.
16. Chen C, Tian X, Zhao X, et al. Clinical study of serum IGFBP7 in predicting lymphatic metastasis in patients with lung adenocarcinoma. Curr Probl Cancer 2020;44:100584.
17. Yi X, Zheng X, Xu H, et al. IGFBP7 and the Tumor Immune Landscape: A Novel Target for Immunotherapy in Bladder Cancer. Front Immunol 2022;13:898493.
18. Siegel RL, Miller KD, Fuchs HE, et al. Cancer statistics, 2022. CA Cancer J Clin 2022;72:7-33.
19. Sung H, Ferlay J, Siegel RL, et al. Global Cancer Statistics 2020: GLOBOCAN Estimates of Incidence and Mortality Worldwide for 36 Cancers in 185 Countries. CA Cancer J Clin 2021;71:209-49.
20. Liu L, Yang Z, Zhang W, et al. Decreased expression of IGFBP7 was a poor prognosis predictor for gastric cancer patients. Tumour Biol 2014;35:8875-81.
21. Sato Y, Inokuchi M, Takagi Y, et al. Relationship between expression of IGFBP7 and clinicopathological variables in gastric cancer. J Clin Pathol 2015;68:795-801.
22. Zhao Q, Zhao R, Song C, et al. Increased IGFBP7 Expression Correlates with Poor Prognosis and Immune Infiltration in Gastric Cancer. J Cancer 2021;12:1343-55.
23. Vivian J, Rao AA, Nothaft FA, et al. Toil enables reproducible, open source, big biomedical data analyses. Nat Biotechnol 2017;35:314-6.
24. Ru B, Wong CN, Tong Y, et al. TISIDB: an integrated repository portal for tumor-immune system interactions. Bioinformatics 2019;35:4200-2.
25. Yu G, Wang LG, Han Y, et al. clusterProfiler: an R package for comparing biological themes among gene clusters. OMICS 2012;16:284-7.
26. Subramanian A, Tamayo P, Mootha VK, et al. Gene set enrichment analysis: a knowledge-based approach for interpreting genome-wide expression profiles. Proc Natl Acad Sci U S A 2005;102:15545-50.
27. Love MI, Huber W, Anders S. Moderated estimation of fold change and dispersion for RNA-seq data with DESeq2. Genome Biol 2014;15:550.
28. Yao S, He L, Zhang Y, et al. HOXC10 promotes gastric cancer cell invasion and migration via regulation of the NF-κB pathway. Biochem Biophys Res Commun 2018;501:628-35.
29. Chen YR, Li YT, Wang MQ, et al. Prognostic significance and function of MCM10 in human hepatocellular carcinoma. Future Oncol 2021;17:4457-70.
30. Xiong D, Pan J, Yin Y, et al. Novel mutational landscapes and expression signatures of lung squamous cell carcinoma. Oncotarget 2017;9:7424-41.
31. Zhang L, Lian R, Zhao J, et al. IGFBP7 inhibits cell proliferation by suppressing AKT activity and cell cycle progression in thyroid carcinoma. Cell Biosci 2019;9:44.
32. Zhao L, Liang J, Zhong W, et al. Expression and prognostic analysis of BGN in head and neck squamous cell carcinoma. Gene 2022;827:146461.
33. Takeno A, Takemasa I, Doki Y, et al. Integrative approach for differentially overexpressed genes in gastric cancer by combining large-scale gene expression profiling and network analysis. Br J Cancer 2008;99:1307-15.
34. Li D, Xia L, Huang P, et al. Cancer-associated fibroblast-secreted IGFBP7 promotes gastric cancer by enhancing tumor associated macrophage infiltration via FGF2/FGFR1/PI3K/AKT axis. Cell Death Discov 2023;9:17.
35. Kim J, Kim WH, Byeon SJ, et al. Epigenetic Downregulation and Growth Inhibition of IGFBP7 in

Gastric Cancer. Asian Pac J Cancer Prev 2018;19:667-75.
36. Saisana M, Griffin SM, May FE. Importance of the type I insulin-like growth factor receptor in HER2, FGFR2 and MET-unamplified gastric cancer with and without Ras pathway activation. Oncotarget 2016;7:54445-62.
37. Heckl SM, Wiesener V, Behrens HM, et al. The expression of the insulin receptor in gastric cancer correlates with the HER2 status and may have putative therapeutic implications. Gastric Cancer 2019;22:1130-42.
38. Kwon HJ, Park MI, Park SJ, et al. Insulin Resistance Is Associated with Early Gastric Cancer: A Prospective Multicenter Case Control Study. Gut Liver 2019;13:154-60.
39. Saisana M, Griffin SM, May FEB. Insulin and the insulin receptor collaborate to promote human gastric cancer. Gastric Cancer 2022;25:107-23.
40. Liu Q, Jiang J, Zhang X, et al. Comprehensive Analysis of IGFBPs as Biomarkers in Gastric Cancer. Front Oncol 2021;11:723131.
41. Liu CT, Wu FC, Zhuang YX, et al. The diagnostic value of serum insulin-like growth factor binding protein 7 in gastric cancer. PeerJ 2023;11:e15419.
42. Zhang XY, Zhang PY, Aboul-Soud MA. From inflammation to gastric cancer: Role of Helicobacter pylori. Oncol Lett 2017;13:543-8.
43. Eckert RL, Green H. Structure and evolution of the human involucrin gene. Cell 1986;46:583-9.
44. Kawabe K, Nakanuma Y, Terada T, et al. Adenosquamous carcinoma of the stomach presenting "giant gastric folds". Gastroenterol Jpn 1990;25:739-45.
45. Tesfaigzi J, Carlson DM. Expression, regulation, and function of the SPR family of proteins. A review. Cell Biochem Biophys 1999;30:243-65.

Cite this article as: Xu HW, Wang MQ, Zhu SL. Analysis of IGFBP7 expression characteristics in pan-cancer and its clinical relevance to stomach adenocarcinoma. Transl Cancer Res 2023;12(10):2596-2612. doi: 10.21037/tcr-23-1055

Supplementary

Table S1 Abbreviations of cancers in The Cancer Genome Atlas (TCGA)

Abbreviation	Cancer type
ACC	Adrenocortical carcinoma
BLCA	Bladder urothelial carcinoma
BRCA	Breast invasive carcinoma
CESC	Cervical squamous cell carcinoma and endocervical adenocarcinoma
CHOL	Cholangiocarcinoma
COAD	Colon adenocarcinoma
DLBC	Lymphoid neoplasm diffuse large B-cell lymphoma
ESCA	Esophageal carcinoma
GBM	Glioblastoma multiforme
GBMLGG	Glioma
HNSC	Head and neck squamous cell carcinoma
KICH	Kidney chromophobe
KIRC	Kidney renal clear cell carcinoma
KIRP	Kidney renal papillary cell carcinoma
LGG	Brain lower grade glioma
LIHC	Liver hepatocellular carcinoma
LUAD	Lung adenocarcinoma
LUSC	Lung squamous cell carcinoma
MESO	Mesothelioma
OV	Ovarian serous cystadenocarcinoma
PAAD	Pancreatic adenocarcinoma
PCPG	Pheochromocytoma and paraganglioma
PRAD	Prostate adenocarcinoma
READ	Rectum adenocarcinoma
SARC	Sarcoma
SKCM	Skin cutaneous melanoma
STAD	Stomach adenocarcinoma
TGCT	Testicular germ cell tumors
THCA	Thyroid carcinoma
THYM	Thymoma
UCEC	Uterine corpus endometrial carcinoma
UCS	Uterine carcinosarcoma
UVM	Uveal melanoma

https://dx.doi.org/10.21037/tcr-23-1055

Table S2 The results of univariate and multivariate Cox regression analyses conducted to investigate the impact of clinical characteristics on the disease-specific survival (DSS) of stomach adenocarcinoma (STAD) patients

Characteristics	Total (N)	Univariate analysis		Multivariate analysis	
		HR (95% CI)	P value	HR (95% CI)	P value
T stage (T3 and T4 *vs.* T2 and T1)	345	2.089 (1.192–3.660)	0.010	1.290 (0.629–2.646)	0.487
N stage (N1, N2, N3 *vs.* N0)	334	1.807 (1.075–3.036)	0.025	1.134 (0.619–2.078)	0.683
M stage (M1 *vs.* M0)	333	2.438 (1.221–4.870)	0.012	1.865 (0.885–3.928)	0.101
Pathologic stage (II, III, IV *vs.* I)	331	3.259 (1.317–8.065)	0.011	2.616 (0.702–9.741)	0.152
Gender (male *vs.* female)	349	1.573 (0.985–2.514)	0.058	1.703 (1.043–2.782)	0.033
Age (years) (>65 *vs.* ≤65)	346	1.211 (0.797–1.840)	0.371		
Histologic grade (G2, G3 *vs.* G1)	340	2.014 (0.280–14.475)	0.486		
Reflux history (Yes *vs.* No)	208	0.598 (0.272–1.313)	0.200		
H. pylori infection (Yes *vs.* No)	157	0.558 (0.200–1.554)	0.264		

Table S3 The results of univariate and multivariate Cox regression analyses conducted to investigate the impact of clinical characteristics on the progression-free interval (PFI) of stomach adenocarcinoma (STAD) patients

Characteristics	Total (N)	Univariate analysis		Multivariate analysis	
		HR (95% CI)	P value	HR (95% CI)	P value
T stage (T3 and T4 *vs.* T2 and T1)	364	1.705 (1.095–2.654)	0.018	1.245 (0.478–3.245)	0.654
N stage (N1, N2, N3 *vs.* N0)	354	1.640 (1.075–2.501)	0.022	1.529 (0.643–3.636)	0.337
M stage (M1 *vs.* M0)	353	2.224 (1.194–4.144)	0.012	1.718 (0.641–4.607)	0.282
Pathologic stage (II, III, IV *vs.* I)	349	2.547 (1.288–5.039)	0.007	1.385 (0.278–6.891)	0.691
Gender (male *vs.* female)	372	1.638 (1.099–2.440)	0.015	2.484 (1.263–4.885)	0.008
Age (years) (>65 *vs.* ≤65)	369	0.858 (0.603–1.221)	0.395	0.858 (0.603–1.221)	0.395
Histologic grade (G2, G3 *vs.* G1)	363	1.555 (0.384–6.294)	0.536		
Reflux history (Yes *vs.* No)	214	0.482 (0.232–1.000)	0.050	0.504 (0.190–1.338)	0.169
H. pylori infection (Yes *vs.* No)	163	0.321 (0.100–1.024)	0.055	0.352 (0.107–1.161)	0.087

https://dx.doi.org/10.21037/tcr-23-1055

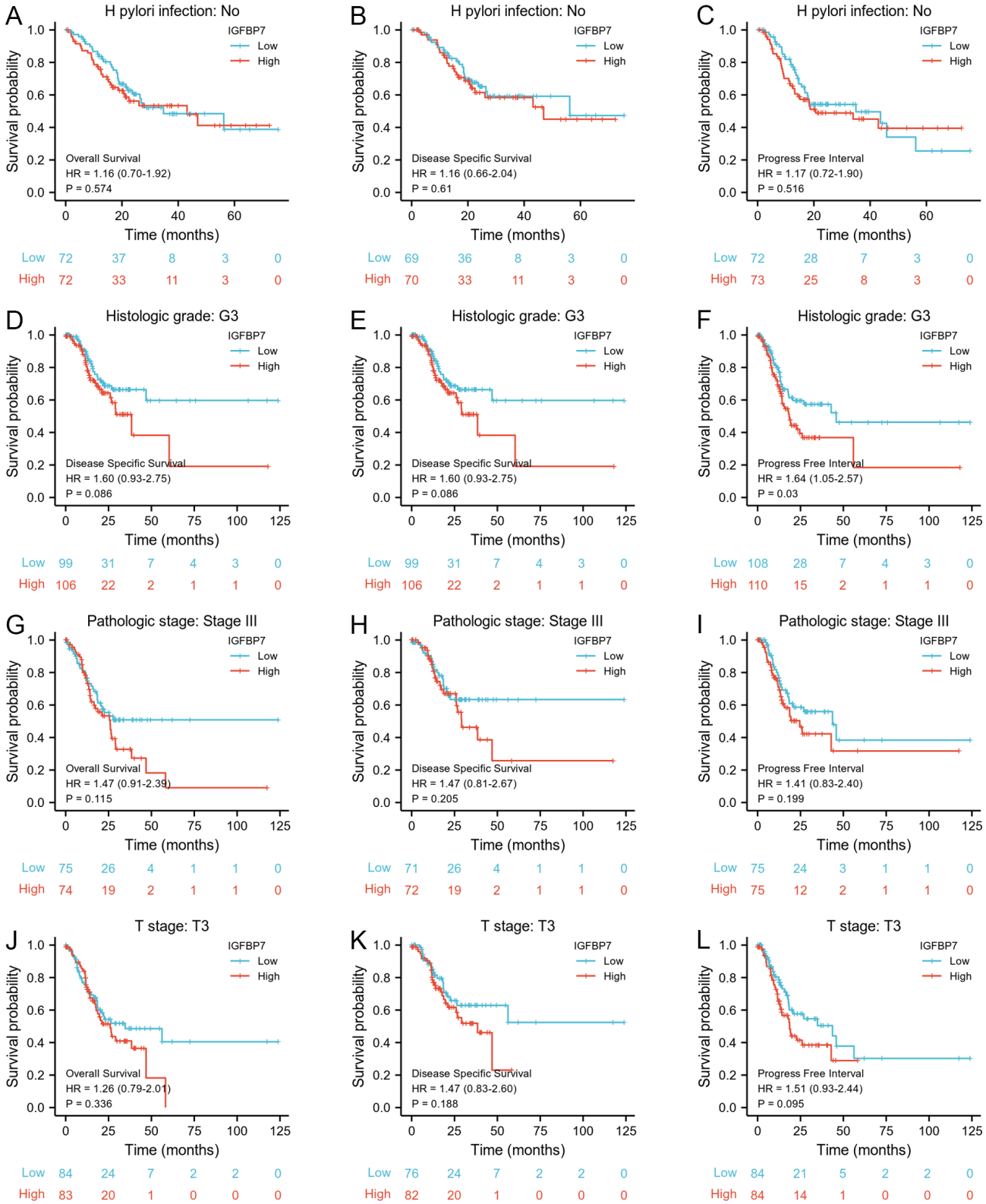

Figure S1 The correlations of IGFBP7 expression with prognosis among four clinical subgroups of stomach adenocarcinoma (STAD).

https://dx.doi.org/10.21037/tcr-23-1055

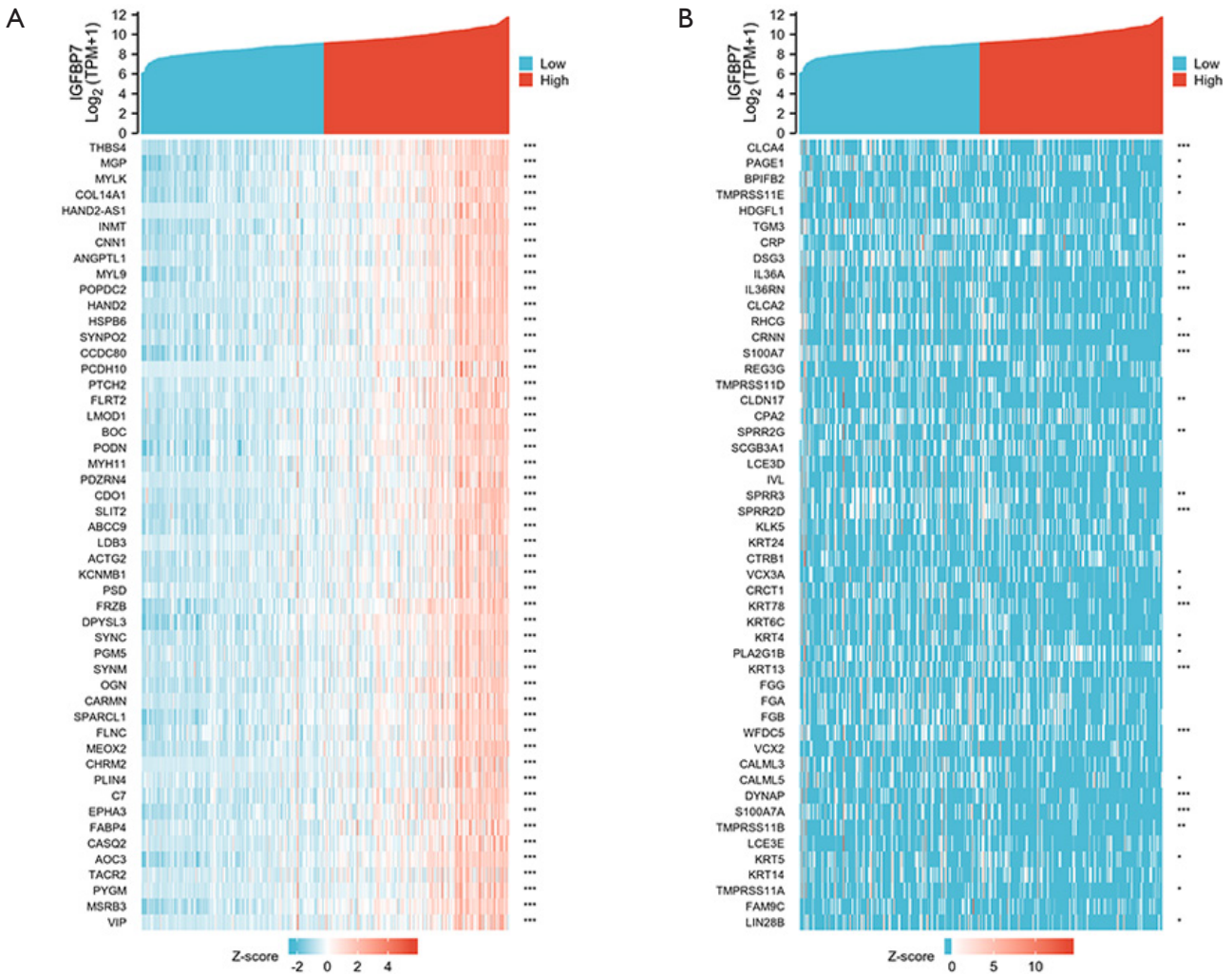

Figure S2 The heat-map displays the top 50 genes that positively (A) or negatively (B) correlated with IGFBP7 expression in stomach adenocarcinoma (STAD). ns, not significant, P≥0.05; *, P<0.05; **, P<0.01; ***, P<0.001.

https://dx.doi.org/10.21037/tcr-23-1055